STEM CELLS AND DEVELOPMENT
Volume 25, Number 17, 2016
© Mary Ann Liebert, Inc.
DOI: 10.1089/scd.2016.0093

microRNA-145 Mediates the Inhibitory Effect of Adipose Tissue-Derived Stromal Cells on Prostate Cancer

Kiyoshi Takahara,[1] Masaaki Ii,[2,3] Teruo Inamoto,[1] Takatoshi Nakagawa,[2] Naokazu Ibuki,[1] Yuki Yoshikawa,[1] Takuya Tsujino,[1] Taizo Uchimoto,[1] Kenkichi Saito,[1] Tomoaki Takai,[1] Naoki Tanda,[1] Koichiro Minami,[1] Hirofumi Uehara,[1] Kazumasa Komura,[1] Hajime Hirano,[1] Hayahito Nomi,[1] Satoshi Kiyama,[1] Michio Asahi,[2] and Haruhito Azuma[1]

Adipose-derived stromal cell (ASC), known as one of the mesenchymal stem cells (MSCs), is a promising tool for regenerative medicine; however, the effect of ASCs on tumor growth has not been studied sufficiently. We investigated the hypothesis that ASCs have an inhibitory effect on metastatic tumor progression. To evaluate the in vitro inhibitory effect of ASCs on metastatic prostate cancer (PCa), direct coculture and indirect separate culture experiments with PC3M-luc2 cells and human ASCs were performed, and ASCs were administered to PC3M-luc2 cell-derived tumor-bearing nude mice for in vivo experiment. We also performed exosome microRNA (miRNA) array analysis to explore a mechanistic insight into the effect of ASCs on PCa cell proliferation/apoptosis. Both in vitro and in vivo experiments exhibited the inhibitory effect of ASCs on PC3M-luc2 cell proliferation, inducing apoptosis and PCa growth, respectively. Among upregulated miRNAs in ASCs compared with fibroblasts, we focused on miR-145, which was known as a tumor suppressor. ASC-derived conditioned medium (CM) significantly inhibited PC3M-luc2 cell proliferation, inducing apoptosis, but the effect was canceled by miR-145 knockdown in ASCs. ASC miR-145 knockdown CM also reduced the expression of Caspase 3/7 with increased antiapoptotic protein, BclxL, expression in PC3M-luc2 cells. This study provides preclinical data that ASCs inhibit PCa growth, inducing PCa cell apoptosis with reduced activity of BclxL, at least in part, by miR-145, including exosomes released from ASCs, suggesting that ASC administration could be a novel and promising therapeutic strategy in patients with PCa.

Introduction

Most of PCa patients are cured with surgery and/or radiation therapy; however, more than 30%–40% of patients will eventually progress and develop advanced disease. While androgen ablation prolongs life with advanced PCa, remissions are temporary because surviving tumor cells progress to establish castration-resistant PCa (CRPC). Identifying targetable mechanisms underlying CRPC progression is essential for improving survival of PCa patients with advanced disease. The premise is that development of CRPC results from adaptive upregulation of antiapoptotic genes, acquisition of gonadal testosterone-independent AR activation, and activation of alternative growth factor signaling events as a consequence of selective pressures of treatment. Moreover, the mandate to modern PCa research is to establish diagnostic parameters that identify and predict the natural history of different subclasses of disease to affect appropriate therapeutic strategies for individual PCa patients.

Since adipose tissue represents an abundant and accessible source of adult stem cells with the ability to differentiate along multiple lineages, adipose tissue-derived stromal cells (ASCs) are considered a great alternative source of mesenchymal stem cells (MSCs). ASCs exhibit properties that are similar to MSCs, an adult stem cell type [1]. In 2005, the Mesenchymal and Tissue Stem Cell Committee of the International Society for Cellular Therapy established the minimal criteria for MSC definition. Three criteria were proposed: adherence to plastic, specific surface antigen (CD73+, CD90+, CD105+, CD45−, CD34−, CD14 or CD11b−, CD79− or CD19−, HLA-DR), and in vitro capability to give rise to adipocytes, osteoblasts, and chondrocytes [2].

Recent studies have linked ASCs to cancer development. An in vivo murine model demonstrated that ASCs home to tumor sites when injected intravenously, and the stromal-derived growth factor-1 (SDF-1)/CXC receptor 4 (CXCR4) axis plays an important role in mediating the tumor-promoting effect of ASCs [3]. Walter et al. reported that interleukin 6

Departments of [1]Urology and [2]Pharmacology, Faculty of Medicine, Osaka Medical College, Osaka, Japan.
[3]Division of Research Animal Laboratory and Translational Medicine, Research and Development Center, Osaka Medical College, Osaka, Japan.

(IL-6) secreted by ASCs is related to the migration and invasion of breast tumor cells [4]. IL-6 plays as a critical growth factor for several types of cancer, including multiple myeloma and PCa [5]. Another report indicated that ASCs had a promotional effect on the proliferation of PCa cells in an in vivo xenograft model [6]. On the other hand, several studies have indicated the negative effect on tumor cells. Cousin et al. have reported that ASCs exhibited a suppressive effect on the proliferation of pancreatic cancer cells under coculture condition [7], and Sun et al. demonstrated that implanted ASCs inhibited breast cancer metastasis and growth in a murine model [8]. Moreover, the ability of ASCs to specifically localize multiple tumors makes them extremely attractive for targeted cancer therapy [9]. Despite the above controversial issues, genetically modified ASCs have demonstrated the safe use for cancer treatment using murine xenograft models [10–12].

We have previously reported that ASCs directly inhibited the proliferation of two different types of PCa cells, androgen-responsive (LNCaP) and androgen-nonresponsive (PC3) cells, through apoptosis both in vitro and in vivo, and that the antiproliferative effect of ASCs on PCa cells appears to be mediated, at least in part, by TGF-β1 secretion and signaling [13]. Since ASCs are easily obtainable from adipose tissue and can be quickly expanded to the desired number in culture, we suggested that ASC transplantation in patients with PCa should be optimized before starting clinical trials.

In the present study, to elucidate further mechanism for ASC-induced negative effect on PCa functions, especially targeting on the metastasis and invasion of PCa, we carried out in vitro and in vivo studies using a luciferase-expressing metastatic PCa cell line, which was stably transfected with the firefly luciferase gene (luc2), PC3M-luc2, originated from androgen-nonresponsive human PCa cells, PC3, with human ASCs under direct coculture and indirect separate culture conditions. We also performed exosome microRNA (miRNA) array analysis to gain a mechanistic insight into the effect of ASCs on PCa cell proliferation/apoptosis.

Materials and Methods

Cell lines

PC3M-luc2, originated from PC3 (which is an androgen-independent cell line), is a luciferase-expressing metastatic PCa cell line, which was stably transfected with the firefly luciferase gene (luc2), and was purchased from Caliper Life-Science (Hopkinton, MA). This cell was maintained in RPMI1640 supplemented with 10% fetal bovine serum (FBS) and 1% penicillin/streptomycin (Life Technologies, Burlington, Canada). Since it was difficult to isolate enough number of ASCs in elderly men who underwent some hormonal or chemotherapy for prostate cancer, ASCs isolated from subcutaneous adipose tissue of a 52-year-old female donor were purchased from Lonza (Lonza, Inc., Walkersville, MD) and maintained in MesenPRO RS™ Medium with L-glutamine 2 mM and 1% antibiotic–antimycotic mix (Life Technologies). ASCs were consistent with the criteria described above in the Introduction section and were used under passage 3 for experiments. Normal human dermal fibroblasts (NHDFs) isolated from a 50-year-old male donor were obtained from Lonza and cultured in fibroblast growth medium-2 (FGM-2) containing FBM, 0.1% insulin, 0.1% recombinant human fibroblast growth factor-B, 0.1% GA-1000, and 2% FBS (Lonza). Cells were grown at 37°C and 5% CO_2. Since NHDFs are well known as one of the important factors that affect the microenvironment surrounding cancer cells, we used NHDFs not only for the simple control cells of ASCs but also for exploring the relationship between NHDFs and PCa cells in carcinogenesis in this study as well as in our previous study [13].

Assessment of tumor growth

All animal procedures were performed according to the guidelines of the Osaka Medical College Animal Care and Use Committee. PC3M-luc2 cells (1×10^6) with 50 μL of Matrigel™ (Becton Dickinson Labware, Franklin Lakes, NJ) and 50 μL of serum-free RPMI1640 were injected intraperitoneally into 6–8-week-old male athymic nude mice to make a peritoneal metastasis model. The cell injection day of PC3M-luc2 was taken as the starting point and defined as day 0. At week 2 after the injection of PC3M-luc2 cells, the mice were then injected intraperitoneally with 15 mg/mL/kg luciferin (Calipers Life Sciences), and 2 min after, the bioluminescent (BLI) signals of the injected cells were measured using Photon Imager (BIOSPACE LAB, Paris, France). Mice with solid tumors formed in the intraperitoneal space were randomly assigned in two groups: one was treated with NHDFs (1×10^5) with 100 μL of PBS, and the other was treated with ASCs (1×10^5) with 100 μL of PBS. Both cells were injected intraperitoneally once a week, and BLI measurements were also performed once a week from 2 to 6 weeks. Body weight measurements were carried out twice a week. At week 6, the treatment was stopped, and all the mice were sacrificed, and tumor tissue were harvested and immediately frozen with O.C.T.™ compound (Sakura Finetek Japan, Tokyo, Japan) for histological examination.

Histological examination

For immunohistochemistry, tissues were embedded in O.C.T. compound and snap-frozen in liquid nitrogen. Frozen sections, 6 μm thick, were mounted on silane-coated glass slides and air-dried for 1 h. Cell apoptosis was confirmed by detection of fragmented DNA, using a DeadEnd™ Colorimetric TUNEL System (Promega, Madison, WI) in accordance with the manufacturer's instructions. As markers of cell proliferation, sections were stained with anti-Human Ki-67 eFluor® 570 (eBioscience, Frankfurt, Germany; 1:200) and anti-SMα-actin (Sigma-Aldrich Japan K.K., Tokyo, Japan; 1:500). Nuclear counterstaining was performed by incubation with 4′,6-diamidino-2-phenylindole (DAPI) solution (Sigma-Aldrich; 1 μg/mL in PBS) for 10 min at room temperature. Double-positive cells for Ki-67 and DAPI staining were counted with multichannel systems in a computer-assisted fluorescent/light microscope BioZero BZ-8000 (Keyence, Osaka, Japan) and averaged for quantitative analysis.

Cell proliferation assay

PC3M-luc2 cell proliferation activity was evaluated using both coculture and separated culture of ASCs versus NHDFs. For coculture assays, PC3M-luc2 cells were cocultured with ASCs or NHDF cells labeled with CM-DiI (Life Technologies) according to the manufacturer's instructions and conditions of our previous study [13]. PC3M-luc2 cells (total 2.5×10^5, $1.2\times10^2/mm^2$) at different ratios (3:1 or 1:1 with ASCs/NHDF,

respectively) were cultured in complete RPMI medium. After 48 h, cells were measured by direct cell counting under a computer-assisted fluorescent/light microscope BioZero BZ-8000. For cell viability assay, PC3M-luc2 cells (5×10^3, 1.5×10^2/mm^2) were first plated in cell culture inserts with a Transwell 24-well plate (0.4-μm pore size) (Corning, NY) in complete medium overnight. Then, cells were transferred to a new Transwell 24-well plate in the presence of ASCs or NHDF conditioned medium (CM) for another 48 h. Cell viability was measured by the MTT cell growth assay kit, according to the manufacturer's instructions (Millipore, Billerica, MA).

Apoptosis assay

ASC- or NHDF-induced apoptosis in PC3M-luc2 cells was assessed using an APO Percentage™ apoptosis assay kit (Biocolor Ltd., Belfast, United Kingdom). PC3M-luc2 cells (5×10^3, 1.5×10^2/mm^2) were first plated in cell culture inserts with a Transwell 24-well plate (0.4-μm pore size) in complete medium overnight. Then, cells were transferred to a new Transwell 24-well plate in the presence of ASCs or NHDF CM for another 48 h. Then, the medium was discarded, and the cells were incubated with 100 μL of serum-free RPMI1640 containing 5% APO Percentage dye for 30 min. Cell surface-bound dye was extracted by lysis solution and immediately observed under a computer-assisted fluorescent/light microscope BioZero BZ-8000.

Exosome miRNA array

ASCs or NHDFs (2×10^6, 3.6×10^2/mm^2) were first plated in complete medium overnight. Then, cells were incubated with 6 mL of serum-free RPMI1640 for another 48 h. Exosomes were collected from each supernatant using the PureExo® Exosome Isolation kit (101Bio, Palo Alto, CA) following the manufacturer's instructions. Exosomal miRNA expression profiling was performed using Affymetrix GeneChip® miRNA 4.0 arrays (Affymetrix, Santa Clara, CA). The RNA was labeled using the FlashTag™ Biotin HSR RNA Labeling Kit (Affymetrix) and then hybridized to the miRNA array. For scanning the signals and analyzing the data, Affymetrix® Expression Console™ Software 1.2 (Affymetrix) was used for the microarray analysis.

miR-145 detection

ASCs were transfected with miR-145 hairpin inhibitor or negative control purchased from Dharmacon Research (Lafayette, CO) at doses of 0, 10, 50, and 100 nM. Cells were grown for 48 h and miR-145 detection was performed with QuantiGene® ViewRNA miRNA ISH Cell Assay (Affymetrix) according to the manufacturer's protocols. Then, cells were immediately observed under a computer-assisted fluorescent/light microscope BioZero BZ-8000.

Assessment of cell proliferation and apoptosis in PC3M-luc2 after miR-145 knockdown of ASCs

For cell viability assay, PC3M-luc2 cells (5×10^3, 1.5×10^2/mm^2) were first plated in cell culture inserts with a Transwell 24-well plate in complete medium overnight. Then, cells were transferred to a new Transwell 24-well plate for another 48 h in the presence of ASCs after transfection with miR-145 hairpin inhibitor or negative control at doses of 10, 50, and 100 nM. Cell viability was measured by the MTT cell growth assay kit according to the manufacturer's recommendations. Caspase-3/7 activation assay was performed using a Caspase-Glo™ 3/7 assay kit (Promega) in accordance with the manufacturer's instructions. The Caspase-Glo 3/7 reagent was then added to each well, and the plate was incubated at room temperature for 1 h. The luminescence of each sample was measured with the GloMax-Multi + Detection System (Promega).

Western blot analysis

PC3M-luc2 cells were cocultured with ASCs in a Transwell 10-cm dish with 100 nM of miR-145 hairpin inhibitor or negative control for 48 h. The cells on the Transwell insert were collected and lysed using RIPA buffer (25 mM Tris, 0.1 M NaCl, 1% Triton X-100, 0.5% deoxycholic acid, 0.1% SDS, pH 7.4). The lysates were subjected to SDS-PAGE, followed by western blot analysis (Nihon Eido Corp., Tokyo, Japan). The samples were probed with antibodies of interest. The images were captured and analyzed using ChemiDoc (Bio-Rad, Hercules, CA).

Statistical analyses

All values in vitro are presented as mean ± SD, and those in vivo are presented as mean ± SEM. Statistical comparison of results was performed by Student's t test. Western blot analyses were performed twice, and other in vitro experiments were repeated at least in triplicate and analyzed.

Results

ASCs inhibited the progression of PC3M-luc2 cells in vivo

We first evaluated the effects of ASCs on PCa growth in in vivo luciferase assay. At week 2 after the intraperitoneal injection of PC3M-luc2 cells, 14 male athymic mice bearing peritoneal tumor metastasis were randomly divided into two groups. One was treated with NHDFs ($n=7$) and the other was treated with ASCs ($n=7$). Both intraperitoneal injection of NHDFs or ASCs and BLI measurements were performed once a week from 2 to 6 weeks. The percent body weight of each mouse was plotted twice a week from 0 to 6 weeks (Fig. 1A). No significant effect on animal body weight was observed in both groups during the treatment period. Tumor growth rate ($n=7$ in each group, ASCs: −12.6, 3.8, −2.7, −31.9, −19.4, 3.2, and −11.6 and NHDFs: 81.4, 9036.5, 3,626, 3234.9, 14,038, 363.8, and 29,790) is shown in Figure 1B, and those of mice bearing PC3M-luc2 subjected to ASCs were significantly lower compared with NHDFs ($P<0.01$), represented in Photon Imager (Fig. 1C). Consistent with luciferase assay, macroscopic findings demonstrated that PC3M-luc2 cells treated with NHDFs were grown with intraperitoneal lymph node metastasis, while those with ASCs were markedly suppressed (Fig. 1C, white arrows indicate sites of tumor). These findings indicate that local transplantation of ASCs significantly inhibits both metastasis and invasion of PC3M-luc2 cells without any severe adverse events.

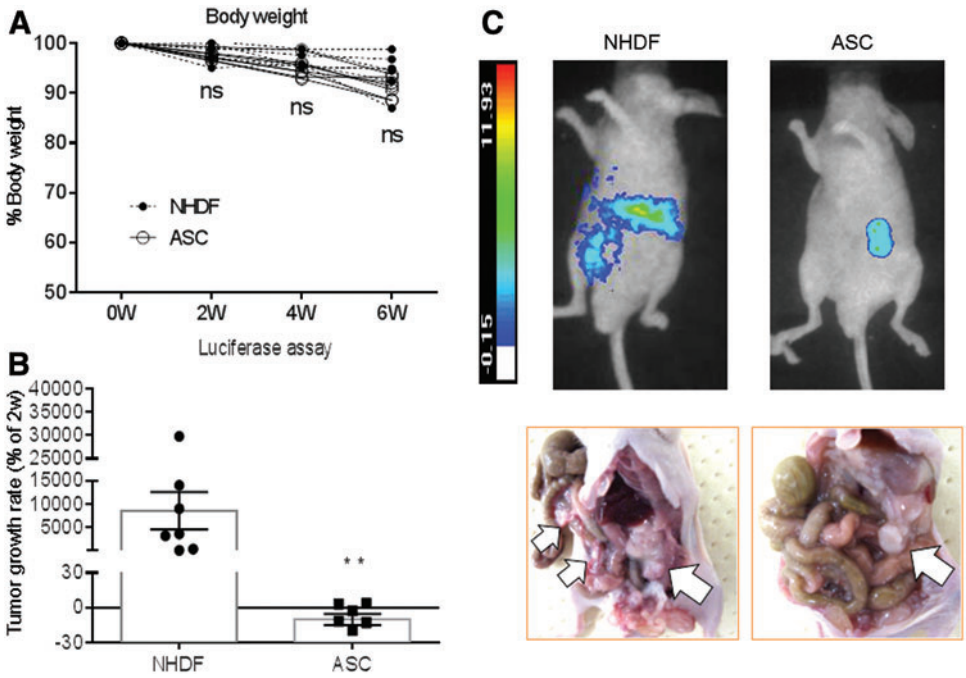

FIG. 1. Effect of ASCs on tumor growth of PC3M-luc2 cells. **(A)** Each body weight of the mice treated with ASCs or NHDFs is shown. Each point represents % of body weight normalized to body weight before treatment (ns, not significant vs. NHDFs). **(B)** Luciferase assay of PC3M-luc2 tumor-bearing mice treated with ASCs or NHDFs. Each point represents % of tumor growth rate normalized to that of week 2. Histograms represent each point and the mean with SEM (**$P < 0.01$ vs. NHDFs). **(C)** Representative Photon Imager and macroscopic findings of mice treated with ASCs or NHDFs at week 6. *White arrows* indicate sites of tumor. ASC, adipose-derived stromal cell; NHDF, normal human dermal fibroblast; SEM, standard error of the mean. Color images available online at www.liebertpub.com/scd

ASCs suppressed the growth of PC3M-luc2 cells inducing apoptosis

Next, to assess how ASCs affected the growth of PC3M-luc2 cells, immunohistochemistry for the proliferation marker, Ki67, and TUNEL staining were performed on PC3M-luc2 specimens of NHDFs and ASCs. Double-positive staining for Ki67 was observed in both groups, without any obvious differences between them, and quantification of Ki67-positive cells also indicated no significant intergroup difference (Fig. 2A). However, the number of apoptotic cells was significantly greater in ASCs than that in NHDFs (5.75 ± 0.94 vs.

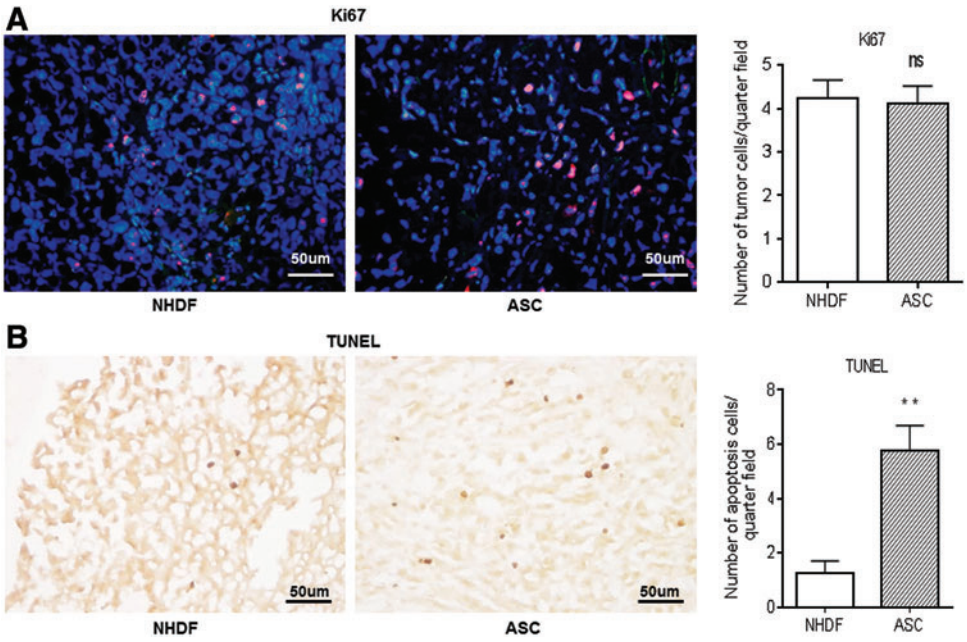

FIG. 2. Ki67 or TUNEL staining on PC3M-luc2 tumor specimens. **(A)** Tissues of mice treated with ASCs or NHDFs were stained with Ki67, SMa-actin, and DAPI. Quantification of Ki67-positive cells is shown. **(B)** Tissues of mice treated with ASCs or NHDFs were stained with TUNEL and the number of apoptotic cells was quantified. Histograms represent the mean with SEM (ns, not significant and **$P < 0.01$ vs. NHDFs). Color images available online at www.liebertpub.com/scd

1.25 ± 0.45, respectively, $P < 0.01$) (Fig. 2B). These IHC studies suggested that ASCs slowed PC3M-luc2 progression, inducing apoptosis.

ASCs inhibited the proliferation of PC3M-luc2 cells in vitro

In parallel with the in vivo experiments that ASCs significantly suppress the growth of PC3M-luc2 cells, we carried out coculture experiments to analyze in vitro growth of PC3M-luc2 cells. PC3M-luc2 cells were cocultured with ASCs or NHDFs at different ratios for 48 h. The result showed that a significant reduction of PC3M-luc2 cell number was observed at both 3:1 and 1:1 ratios with ASCs, while PC3M-luc2 cell number increased when cocultured with NHDFs (Fig. 3A). Next, we examined the proliferation of PC3M-luc2 cells in the presence of CM derived from ASCs or NHDFs using a Transwell™ 24-well plate under direct cell-to-cell contact-free conditions. As shown in Figure 3B, ASC-derived CM significantly inhibited the proliferation/viability of PC3M-luc2 cells compared with NHDF-derived CM. These two in vitro coculture experiments suggested that ASCs inhibited the proliferation of PC3M-luc2 cells regardless of the cell-to-cell contact conditions. Next, to assess how ASCs inhibit the proliferation of PC3M-luc2 cells, in vitro apoptosis assay was performed. Consistent with the in vivo IHC study with TUNEL staining, apoptosis assay with ASC- or NHDF-derived CM indicated that apoptosis was observed more frequently in PC3M-luc2 cells with ASC-CM than with NHDF-derived CM. Quantification of cell apoptosis indicated that the ratio of apoptotic cells (%) was significantly higher for ASCs than for NHDFs in PC3M-luc2 cells (34.83 ± 6.74 vs. 13.49 ± 4.56, respectively, $P < 0.01$) (Fig. 3C). Our in vitro coculture experiments strongly supported our in vivo results and revealed that ASCs significantly suppressed the proliferation of PC3M-luc2 cells, inducing apoptosis.

miR-145 was highly expressed in ASCs

To further elucidate how ASCs negatively influence PC3M-luc2 cell proliferation/viability, we next performed exosome miRNA array analysis with ASCs and NHDFs (Fig. 4). Four miRNAs of miR-4417, miR-7107, miR-1185, and miR-145 whose expression levels were more than fivefold higher in ASCs than in NHDFs are shown in Table 1. Among the above selected miRNAs, we focused on miR-145, which was well known as a tumor suppressor. The expression of miR-145 (miR-145-5p) was high in ASCs compared with NHDFs, and the expression ratio of ASCs/NHDFs was 5.18 (14.86 vs. 2.87).

Hairpin inhibitor reduced miR-145 expression in ASCs

Next, to examine the paracrine tumor-suppressive effect of miR-145 supplied from ASCs, QuantiGene ViewRNA

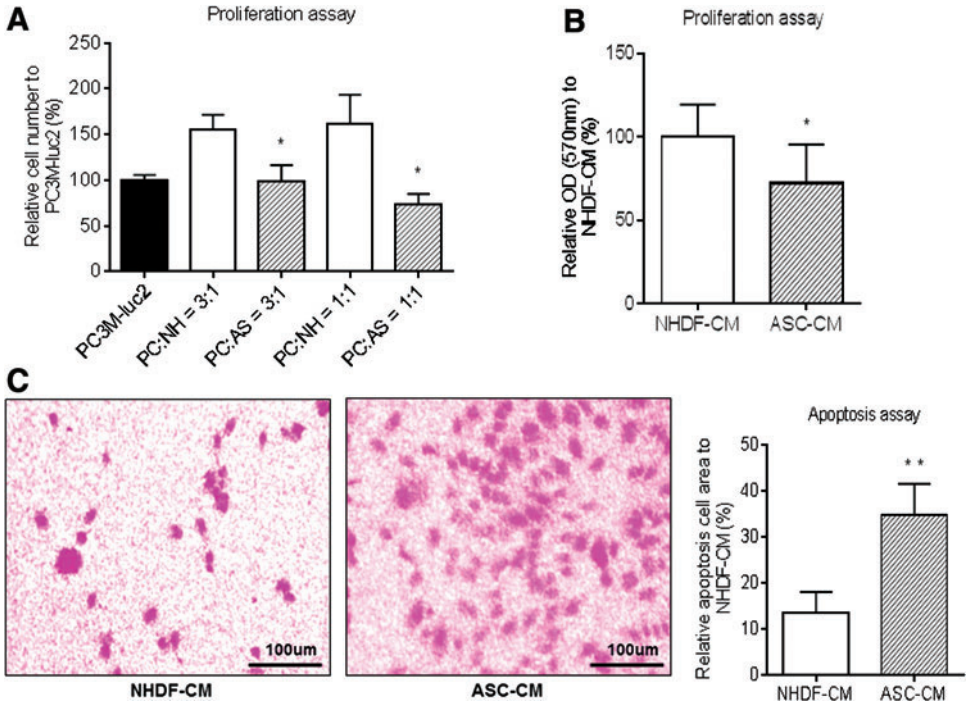

FIG. 3. Effect of ASCs on proliferation activity in PC3M-luc2 cells. **(A)** DiI-PC3M-luc2 cells were cocultured with NHDFs or ASCs at ratios of 1:1 and 3:1. The proliferations were assessed by counting DiI-positive cell number in each experimental group. The percentages of cell number to PC3M-luc2 cells in each group are expressed as relative proliferation activities to PC3M-luc2 cell alone. **(B)** PC3M-luc2 cells were cultured in the presence of ASC- or NHDF-CM under a separate culture condition. Cell viability/proliferation expressed as values at OD of 570 nm wavelength. **(C)** Photomicrographs representing purple stained apoptotic cells in PC3M-luc2 cells with ASC- or NHDF-derived CM (560 PC3M-luc2 cells/field). Percent of apoptotic cell area of PC3M-luc2 cells with ASCs or NHDFs was quantified. Histograms represent the mean with SD. (*$P < 0.05$ vs. NHDFs and **$P < 0.01$ vs. NHDFs). CM, conditioned medium; OD, optical density. Color images available online at www.liebertpub.com/scd

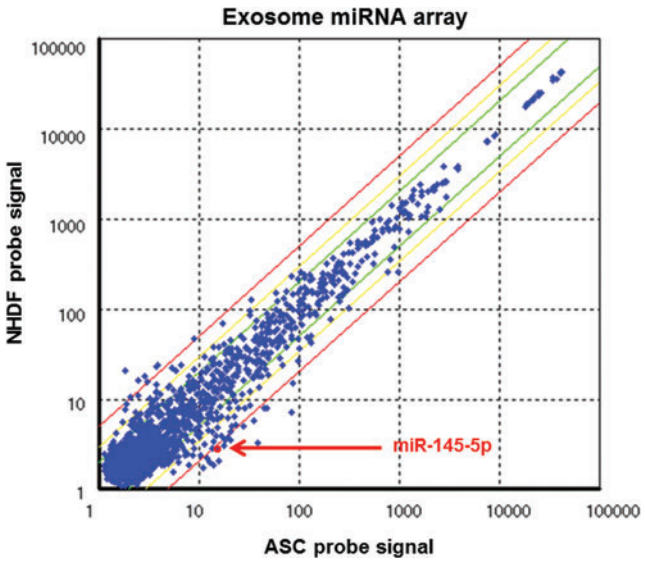

FIG. 4. High expression level of miR-145 in exosome miRNA array analysis. Exosomal miRNA expression of ASCs or NHDFs was examined by Affymetrix GeneChip® miRNA 4.0 arrays (X axis: ASC probe signal, Y axis: NHDF probe signal). *Red arrow* indicates the location of miR-145-5p. Color images available online at www.liebertpub.com/scd

miRNA ISH cell assay was used to quantify knockdown of miR-145 expression in ASCs with miR-145 hairpin inhibitor or the negative control. MiR-145 expression was suppressed ~50% at 10 nM, ~80% at 50 nM, and undetectable at 100 nM after the treatment of miR-145 hairpin inhibitor in ASCs. In contrast, the negative control or Lipofectamine alone suppressed miR-145 expression by less than 20% at maximal doses tested (Fig. 5).

miR-145 knockdown reduced the effect of ASCs on apoptosis and rescued the proliferation in PC3M-luc2 cells

To observe the paracrine tumor-suppressive effect of miR-145 by ASCs, MTT assay, Caspase-3/7 activation assay, and western blot analysis were performed to examine the proliferation of PC3M-luc2 cells in the presence of CM derived from ASCs after the treatment with miR-145 hairpin inhibitor or negative control using a Transwell plate under direct cell-to-cell contact-free conditions. MTT assay indicated that the inhibitory effect of ASCs on PC3M-luc2 cell growth was not observed either at 10 or 50 nM of miR-145 hairpin inhibitor, while after the transfection at 100 nM, the inhibitory effect of ASCs on PC3M-luc2 growth was significantly reduced compared with negative control ($P < 0.05$) (Fig. 6A). Caspase 3/7 expression in the presence of ASC-derived CM after the treatment with miR-145 hairpin inhibitor at 100 nM was significantly decreased in PC3M-luc2 cells compared with negative control at the same concentration (Fig. 6B). Western blot analysis demonstrated that Bcl2 expression in PC3M-luc2 cells in the presence of CM derived from ASCs after the treatment with miR-145 hairpin inhibitor was not affected (1.000 ± 0.00003 in NC and 0.973 ± 0.00223 in miR145 HI), while the expression of the antiapoptotic BclxL protein was significantly increased (1.000 ± 0.0004 in NC and 1.546 ± 0.1772 in miR145 HI) after the treatment with miR-145 hairpin inhibitor compared with negative control (Fig. 7). These in vitro results indicated that ASCs suppressed the growth of PC3M-luc2 cells through the paracrine tumor-suppressive effect of miR-145-induced apoptosis through the caspase-3/7 pathway.

TABLE 1. EXOSOMAL MIRNA EXPRESSION OF ASCS AND NHDFS

Expression ratio (ASC/NHDF)	*ASC*	*NHDF*	*Gene name*
5.82	17.92	3.08	miR-4417
5.79	20.61	3.56	miR-7107-5p
5.28	18.64	3.53	miR-1185-1-3p
5.18	14.86	2.87	miR-145-5p

Four miRNAs whose expression levels were more than fivefold higher in ASCs than in NHDFs are shown.
ASC, adipose-derived stromal cell; NHDF, normal human dermal fibroblast.

Discussion

To establish the personalized medicine for PCa, we have previously demonstrated the antiproliferative effect of ASC

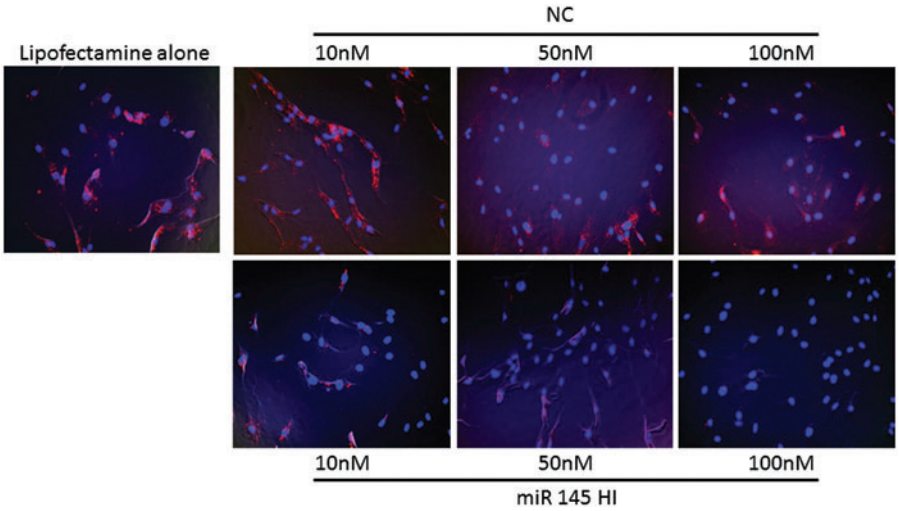

FIG. 5. Knockdown of miR-145 with miR-145 hairpin inhibitor. Representative QuantiGene® ViewRNA miRNA ISH Cell Assay of ASCs transfected with miR-145 hairpin inhibitor (miR 145 HI) or NC at 0, 10, 50, and 100 nM. ASCs were immediately observed under a computer-assisted fluorescent/light microscope BioZero BZ-8000. NC, negative control. Color images available online at www.liebertpub.com/scd

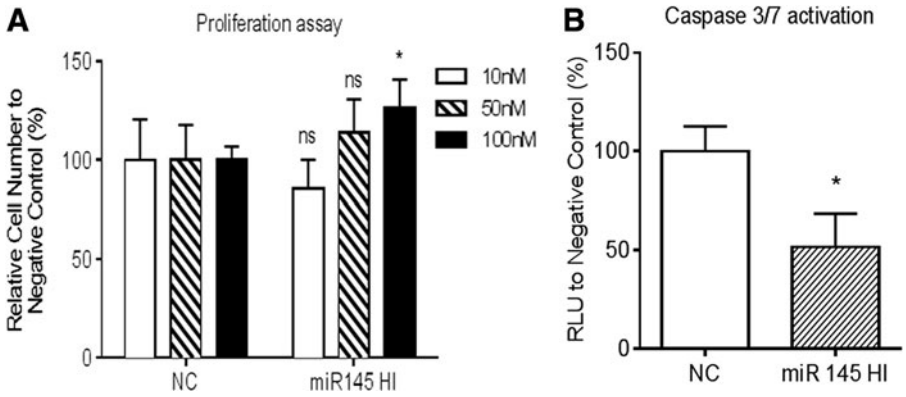

FIG. 6. Effect of miR-145 knockdown of AdSCs in PC3M-luc2 cells. **(A)** PC3M-luc2 cells were cultured in the presence of ADSC-CM transfected with miR-145 hairpin inhibitor (miR 145 HI) or NC at 10, 50, and 100 nM. Cell viability/proliferation was expressed with MTT cell growth assay kit. **(B)** Caspase 3/7 was measured in PC3M-luc2 cells with ASC-CM transfected with miR-145 hairpin inhibitor (miR 145 HI) or NC at 100 nM. RLU of the cells with miR 145 HI to NC was expressed as Caspase 3/7 activity. Histograms represent the mean with SD (ns, not significant and $*P < 0.05$ vs. negative control). RLU, relative luminescence; SD, standard deviation.

transplantation, perhaps through a TGF-β1-dependent signaling pathway in PCa cells [13]. In this study, to further elucidate the role of ASCs on PCa carcinogenesis, including tumor invasion/metastasis, both in vitro and in vivo coculture experiments were carried out using a luciferase-expressing metastatic PCa cell line, PC3M-luc2, originated from androgen-nonresponsive human PCa cells, PC3. In vivo experiments demonstrated that local ASC transplantation suppressed both metastasis and invasion inducing apoptosis following the in vitro results of the antiproliferative effect of ASCs in PC3M-luc2 cells. Next, to gain a mechanistic insight on how ASCs negatively influence PC3M-luc2 cell proliferation/viability, exosome miRNA array analysis with ASCs and NHDFs was performed based on the evidences in which miR-145 was shown to be involved in tumor invasion/metastasis [14–16].

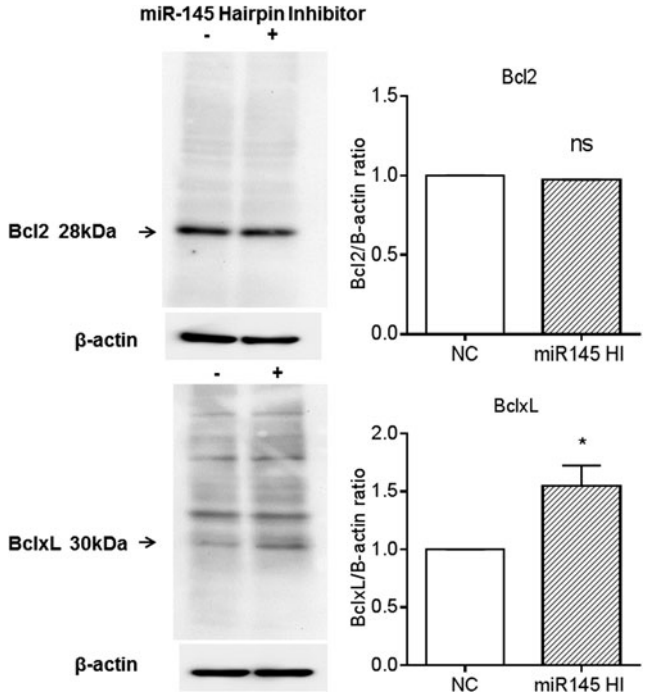

FIG. 7. Increased level of BclxL expression on western blot analysis. Whole cell lysates from PC3M-luc2 cells with ASC-CM transfected with miR-145 hairpin inhibitor (miR 145 HI) or NC at 100 nM and subjected to immunoblotting against Bcl2, BclxL, and β-actin with antibodies. Data are expressed as ratio normalized to β-actin. Histograms represent the mean with SD (ns, not significant and $*P < 0.05$ vs. negative control).

Newly discovered small RNAs are termed microRNAs (miRNAs), which have been defined as a group of endogenous single-stranded noncoding RNAs with a length of 19–25 nucleotides [17–20]. These small RNAs play important roles in numerous cellular processes, including development, proliferation, and apoptosis [21]. miRNAs are frequently misregulated in human cancers [22,23] and can act as either potent oncogenes or tumor suppressor genes [24]. Recently, studies of the regulation of miRNAs in multipotent MSC differentiation have attracted much attention; however, there is hardly any literature that comprehensively and systematically reviews the role of miRNAs in the differentiation of ASCs. Chen et al. first reviewed the molecular mechanisms of miRNAs that both govern and provide a better understanding of molecular events in the differentiation of ASCs and their importance for the development of new strategies in regenerative medicine [25].

The exosome miRNA array analysis demonstrated that the miR-145 expression level was high in ASCs compared with NHDFs. Among the large number of studied miRNAs, hsa-miR-145-5p (miR-145) has a well-characterized tumor suppressor regulatory role in the cell microenvironment [26]. In the context of PCa, miR-145 expression in PCa using clinical specimens was significantly downregulated [27], and Avgeris et al. demonstrated that the loss of the tumor suppressor miR-145 increased the risk for disease progression and predicted the poor survival of PCa patients [28]. Kojima et al. revealed that loss of the miR-143/145 cluster enhanced cancer cell migration and invasion in PCa through directly regulating Golgi membrane protein 1 (GOLM1) [29].

However, the role of miR-145 secreted from ASCs still remains unclear. We then focused on the paracrine tumor-suppressive effect of miR-145 from ASCs in PCa, and in

vitro coculture experiments with knockdown of miR-145 in ASCs using miR-145 hairpin inhibitor were performed. Our coculture results demonstrated that miR-145 was the important factor in ASC-derived CM that induced apoptosis and inhibited the progression of PC3M-luc2 cells. Since we previously demonstrated that ASCs inhibited proliferation activity of the other androgen-dependent PCa cell line, LNCaP, inducing apoptosis [13], ASC-derived miR-145 might also play a key role in the regulation of LNCaP cell viability. Nevertheless, further study with the other cell lines such as LNCaP and androgen receptor-negative hormone-independent DU145 will be required. Regarding possible inhibitory effects of other miRNAs, the exosome miRNA array analysis demonstrated that the expression of miR-4417, miR-7107, and miR-1185 was more than fivefold higher in ASCs than NHDFs as well as miR-145; however, the functions and roles of miRNAs in carcinogenesis have not been elucidated yet, and further investigation would therefore be required to explore their paracrine/inhibitory effects on PCa.

In the present study, we injected five times of ASCs (1×10^5/time), which equal the total number of injected ASCs in our previous study, into PCa-derived peritoneal tumor-bearing mice to demonstrate therapeutic effect; however, since we did not perform the ASC dose-escalation study, the number of ASCs for therapeutic application against cancer should be further optimized in future investigations.

Our previous data suggested that the antiproliferative effect of ASCs on PCa cells appears to be mediated, at least in part, by TGF-β1 secretion and signaling. Interestingly, miR-143 and miR-145, downregulated in PCa, are two miRNAs that are transcribed after TGF-β1 pathway activation [28]. Santos et al. identified that TGF-β1-related miR-143, miR-145, miR-146a, and miR-199a may have a key role in the development of PCa metastasis and restoration of their expression may be a promising therapeutic strategy for PCa treatment [30]. Indeed, previous clinical studies demonstrated that upregulation of TGF-β1 in PCa tissues and high urinary/serum levels of TGF-β1 are associated with enhanced tumor angiogenesis and tumor metastasis, resulting in a poor clinical outcome [31]; however, the tumor-suppressive effect of TGF-β1 through activation of Smad2/3 signaling in PCa cells was reported in a recent article [32], suggesting the controversial role of TGF-β1 in PCa carcinogenesis.

We therefore assume that exogenous TGF-β1 and miR-145 supplied from ASCs could affect the environment of endogenous TGF-β1 signaling and miR-145 in the PCa tumor, inducing apoptosis through the caspase-3/7 pathway. Several pathways contribute to apoptosis and the well-characterized ones are the Akt/PKB pathway, RTKN/NF-κB survival pathway, and p53-mediated apoptosis pathway [33–35]. RTKN was confirmed as a direct target of miR-145 in MCF-7 cells [36] and further enhanced the expression of BclxL by activating NF-κB [34]. These previous reports strongly supported our in vitro coculture results that ASCs suppressed the growth of PC3M-luc2 cells through the paracrine tumor-suppressive effect of miR-145, inducing apoptosis with antiapoptotic activity of BclxL.

In conclusion, this study may provide preclinical proof-of-principle data in which ASCs have been shown to inhibit PCa growth both in vitro and in vivo by induction of apoptosis, at least in part, with miR-145 secretion from ASCs. Moreover, our results that ASCs isolated from a female donor slowed PCa progression give a significant impact on the allogeneic stem cell therapy. For clinical study, the protocol, including the number of ASCs and frequency of administration, should be optimized. Nevertheless, we suggest that allogeneic ASC transplantation might be a promising new therapeutic approach for patients with PCa.

Acknowledgments

The authors thank Teruo Ueno, Rintaro Oide, and Eiko Kohbayashi for their excellent technical assistance. This study was supported, in part, by a grant-in-aid for scientific research from the Ministry of Education, Science, Sports, and Culture of Japan.

Author Disclosure Statement

No competing financial interests exist.

References

1. Gimble JM, AJ Katz and BA Bunnell. (2007). Adipose-derived stem cells for regenerative medicine. Circ Res 100:1249–1260.
2. Vilalta M, IR Degano, J Bago, E Aguilar, SS Gambhir, N Rubio and J Blanco. (2009). Human adipose tissue-derived mesenchymal stromal cells as vehicles for tumor bystander effect: a model based on bioluminescence imaging. Gene Ther 16:547–557.
3. Muehlberg FL, YH Song, A Krohn, SP Pinilla, LH Droll, X Leng, M Seidensticker, J Ricke, AM Altman, et al. (2009). Tissue-resident stem cells promote breast cancer growth and metastasis. Carcinogenesis 30:589–597.
4. Walter M, S Liang, S Ghosh, PJ Hornsby and R Li. (2009). Interleukin 6 secreted from adipose stromal cells promotes migration and invasion of breast cancer cells. Oncogene 28:2745–2755.
5. Smith PC, A Hobisch, DL Lin, Z Culig and ET Keller. (2001). Interleukin-6 and prostate cancer progression. Cytokine Growth Factor Rev 12:33–40.
6. Prantl L, F Muehlberg, NM Navone, YH Song, J Vykoukal, CJ Logothetis and EU Alt. (2010). Adipose tissue-derived stem cells promote prostate tumor growth. Prostate 70: 1709–1715.
7. Cousin B, E Ravet, S Poglio, F De Toni, M Bertuzzi, H Lulka, I Touil, M Andre, JL Grolleau, et al. (2009). Adult stromal cells derived from human adipose tissue provoke pancreatic cancer cell death both in vitro and in vivo. PLoS One 4:e6278.
8. Sun B, KH Roh, JR Park, SR Lee, SB Park, JW Jung, SK Kang, YS Lee and KS Kang. (2009). Therapeutic potential of mesenchymal stromal cells in a mouse breast cancer metastasis model. Cytotherapy 11:289–298; 1p following 298.
9. Uchibori R, T Tsukahara, H Mizuguchi, Y Saga, M Urabe, H Mizukami, A Kume and K Ozawa. (2013). NF-kappaB activity regulates mesenchymal stem cell accumulation at tumor sites. Cancer Res 73:364–372.
10. Grisendi G, R Bussolari, L Cafarelli, I Petak, V Rasini, E Veronesi, G De Santis, C Spano, M Tagliazzucchi, et al. (2010). Adipose-derived mesenchymal stem cells as stable source of tumor necrosis factor-related apoptosis-inducing ligand delivery for cancer therapy. Cancer Res 70:3718–3729.
11. Kucerova L, V Altanerova, M Matuskova, S Tyciakova and C Altaner. (2007). Adipose tissue-derived human mesen-

chymal stem cells mediated prodrug cancer gene therapy. Cancer Res 67:6304–6313.
12. Tyciakova S, M Matuskova, R Bohovic, K Polakova, L Toro, S Skolekova and L Kucerova. (2015). Genetically engineered mesenchymal stromal cells producing TNFalpha have tumour suppressing effect on human melanoma xenograft. J Gene Med 17:54–67.
13. Takahara K, M Ii, T Inamoto, K Komura, N Ibuki, K Minami, H Uehara, H Hirano, H Nomi, et al. (2014). Adipose-derived stromal cells inhibit prostate cancer cell proliferation inducing apoptosis. Biochem Biophys Res Commun 446:1102–1107.
14. Guo W, D Ren, X Chen, X Tu, S Huang, M Wang, L Song, X Zou and X Peng. (2013). HEF1 promotes epithelial mesenchymal transition and bone invasion in prostate cancer under the regulation of microRNA-145. J Cell Biochem 114:1606–1615.
15. Ren D, M Wang, W Guo, X Zhao, X Tu, S Huang, X Zou and X Peng. (2013). Wild-type p53 suppresses the epithelial-mesenchymal transition and stemness in PC-3 prostate cancer cells by modulating miR145. Int J Oncol 42:1473–1481.
16. Wu D, M Li, L Wang, Y Zhou, J Zhou, H Pan and P Qu. (2014). microRNA145 inhibits cell proliferation, migration and invasion by targeting matrix metallopeptidase-11 in renal cell carcinoma. Mol Med Rep 10:393–398.
17. Gangaraju VK and H Lin. (2009). MicroRNAs: key regulators of stem cells. Nat Rev Mol Cell Biol 10:116–125.
18. Hwang HW and JT Mendell. (2006). MicroRNAs in cell proliferation, cell death, and tumorigenesis. Br J Cancer 94:776–780.
19. Lakshmipathy U and RP Hart. (2008). Concise review: microRNA expression in multipotent mesenchymal stromal cells. Stem Cells 26:356–363.
20. Liu SP, RH Fu, HH Yu, KW Li, CH Tsai, WC Shyu and SZ Lin. (2009). MicroRNAs regulation modulated self-renewal and lineage differentiation of stem cells. Cell Transplant 18:1039–1045.
21. Carrington JC and V Ambros. (2003). Role of microRNAs in plant and animal development. Science 301:336–338.
22. Lu J, G Getz, EA Miska, E Alvarez-Saavedra, J Lamb, D Peck, A Sweet-Cordero, BL Ebert, RH Mak, et al. (2005). microRNA expression profiles classify human cancers. Nature 435:834–838.
23. Volinia S, GA Calin, CG Liu, S Ambs, A Cimmino, F Petrocca, R Visone, M Iorio, C Roldo, et al. (2006). A microRNA expression signature of human solid tumors defines cancer gene targets. Proc Natl Acad Sci U S A 103:2257–2261.
24. Esquela-Kerscher A and FJ Slack. (2006). Oncomirs—microRNAs with a role in cancer. Nat Rev Cancer 6:259–269.
25. Chen J, S Deng, S Zhang, Z Chen, S Wu, X Cai, X Yang, B Guo and Q Peng. (2014). The role of miRNAs in the differentiation of adipose-derived stem cells. Curr Stem Cell Res Ther 9:268–279.
26. Sachdeva M and YY Mo. (2010). miR-145-mediated suppression of cell growth, invasion and metastasis. Am J Transl Res 2:170–180.
27. Fuse M, S Kojima, H Enokida, T Chiyomaru, H Yoshino, N Nohata, T Kinoshita, S Sakamoto, Y Naya, et al. (2012). Tumor suppressive microRNAs (miR-222 and miR-31) regulate molecular pathways based on microRNA expression signature in prostate cancer. J Hum Genet 57:691–699.
28. Avgeris M, K Stravodimos, EG Fragoulis and A Scorilas. (2013). The loss of the tumour-suppressor miR-145 results in the shorter disease-free survival of prostate cancer patients. Br J Cancer 108:2573–2581.
29. Kojima S, H Enokida, H Yoshino, T Itesako, T Chiyomaru, T Kinoshita, M Fuse, R Nishikawa, Y Goto, et al. (2014). The tumor-suppressive microRNA-143/145 cluster inhibits cell migration and invasion by targeting GOLM1 in prostate cancer. J Hum Genet 59:78–87.
30. Santos JI, AL Teixeira, F Dias, M Gomes, A Nogueira, J Assis and R Medeiros. (2014). Restoring TGFbeta1 pathway-related microRNAs: possible impact in metastatic prostate cancer development. Tumour Biol 35:6245–6253.
31. Weissert R, A Melms and H Link. (1997). Altered tumor growth factor beta mRNA expression is associated with thymectomy-related clinical remission in myasthenia gravis. J Neurol Sci 151:49–55.
32. Miles FL, NS Tung, AA Aguiar, S Kurtoglu and RA Sikes. (2012). Increased TGF-beta1-mediated suppression of growth and motility in castrate-resistant prostate cancer cells is consistent with Smad2/3 signaling. Prostate 72:1339–1350.
33. Hengartner MO. (2000). The biochemistry of apoptosis. Nature 407:770–776.
34. Liu CA, MJ Wang, CW Chi, CW Wu and JY Chen. (2004). Rho/Rhotekin-mediated NF-kappaB activation confers resistance to apoptosis. Oncogene 23:8731–8742.
35. Raver-Shapira N, E Marciano, E Meiri, Y Spector, N Rosenfeld, N Moskovits, Z Bentwich and M Oren. (2007). Transcriptional activation of miR-34a contributes to p53-mediated apoptosis. Mol Cell 26:731–743.
36. Wang S, C Bian, Z Yang, Y Bo, J Li, L Zeng, H Zhou and RC Zhao. (2009). miR-145 inhibits breast cancer cell growth through RTKN. Int J Oncol 34:1461–1466.

Address correspondence to:
Masaaki Ii, MD, PhD
Division of Research Animal Laboratory and Translational Medicine
Research and Development Center
Osaka Medical College
2-7 Daigaku-machi
Takatsuki
Osaka 569-8686
Japan

E-mail: masaii@osaka-med.ac.jp

Received for publication April 23, 2016
Accepted after revision July 27, 2016
Prepublished on Liebert Instant Online July 27, 2016